15

The electromagnetic calorimeter first level trigger system of the COMET experiment

© L.B. Epshteyn,[1,2] D.N. Grigoriev,[1,2] D.V. Shoukavy[3]

[1]Budker Institute of Nuclear Physics, Siberian Branch, Russian Academy of Sciences,
630090 Novosibirsk, Russia
[2]Novosibirsk State Technical University,
630073 Novosibirsk, Russia
[3]B.I.Stepanov Institute of Physics of the National Academy of Sciences of Belarus,
220072 Minsk, Belarus
e-mail: L.B.Epshteyn@inp.nsk.su

Received March 17, 2025
Revised May 14, 2025
Accepted May 20, 2025

The first level trigger system of the COMET electromagnetic calorimeter, which performs real-time analysis of calorimeter data, is described. Experimental measurements were carried out on the electron beam of the first level trigger system equipment using the proposed algorithm: the overall efficiency at energy release above 30 MeV was 99.4 %, above 40 MeV — 99.7 %, and the own energy resolution of the first level trigger system was better than 5 % for registered signal events (electrons with an energy of 105 MeV). The trigger signal latency measurements between event generation time and its arrival at the digitizing boards measuring channels were made.

Keywords: Trigger system, trigger algorithm, clustering algorithm, digital signal processing, electronics.

DOI: 10.61011/TP.2025.11.62247.38-25

Introduction

The main purpose of the COMET experiment [1–3] is to find coherent muon-to-electron conversion in the nucleus region without neutrino radiation an with single event sensitivity (SES) $\sim 3 \cdot 10^{-17}$.

The desired $\mu^- \mathrm{N} \to e^- \mathrm{N}$ process is actually a two-particle one where the signal electron energy is fixed. For an aluminum target used in this experiment, the signal electron energy is equal to:

$$E_{\mu-e} = (m_\mu - B_\mu - E_{recoil}) = 104.97\,\mathrm{MeV},$$

where m_μ is the muon weight, B_μ is the material-depending binding energy of a muon atom in the 1S state, E_{recoil} is the nucleus recoil energy.

The COMET experiment detector (Figure 1) consists of drift-tube coordinate system *2* and electromagnetic calorimeter *3* consisting of scintillation crystals placed in a longitudinal magnetic field of superconducting solenoid *4*. The drift tube system is designed for precise pulse measurement, which is used to separate signal events with a fixed pulse from background events with continuous pulse distribution. Using the information about specific energy loss (dE/dx) acquired from the drift tube system together with the information (provided from the calorimeter) about the relation between the cluster energy in the track-associated electromagnetic calorimeter and the track pulse (E/p), the system is additionally used for particle type identification. And, since the physical background is nonrelativistic, there will be great differences in dE/dx and E/p depending on the type of particles.

The main purpose of the electromagnetic calorimeter is the generation of a detector trigger signal, and the amount of energy release is the primary argument for decision making because the main background event have an energy lower than that of signal events. To ensure allowable detector trigger frequency, real-time energy resolution shall be at least 5 %. In addition, a real-time data pipeline analysis algorithm without dead time shall be used because the

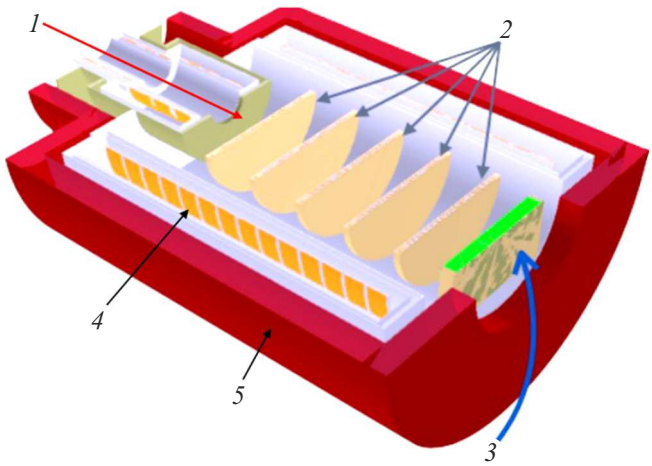

Figure 1. Detector section of the COMET experiment: *1* — electron beam, *2* — drift-tube coordinate system, *3* — electromagnetic calorimeter, *4* — detector solenoid, *5* — yoke.

loading frequency may vary. It shall also consider both statistical fluctuations of electromagnetic shower development and high background loading, i.e. handle compact crystal groups.

The real-time signal processing procedure and detector trigger signal generation are technically implemented in the ECal Pretrigger system.

1. Electromagnetic calorimeter

Electromagnetic calorimeter is based on scintillation crystals. The electromagnetic calorimeter crystals shall have high light yield and also fast response facilitating the signal overlapping reduction. Based on all parameters, a decision was made to use $Lu_{2(1-x)}Y_{2x}SiO_5(Ce)$ (LYSO) crystals for the electromagnetic calorimeter [4]. Energy release with intrinsic crystal radioactivity is lower than electronic noise and therefore its influence is negligible. Electromagnetic calorimeter consists of crystals with a cross-section of 2×2 cm (~ 1 Moliere radius) and a length of 12 cm (10.5 radiation lengths). Electromagnetic calorimeter covers the region inscribed in a circle with a radius of 50 cm and consists of 1920 crystals, which are assembled in modules for ease of mounting.

Schematic diagram of the electromagnetic calorimeter is shown in Figure 2.

2×2 crystal modules (Figure 3) are the main structural component of the electromagnetic calorimeter. When a particle arrives, energy release is distributed between several crystals, therefore to reduce the amount of information to be sent to the pre-trigger system, analog summation from four crystals of one 2×2 module was performed in custom-designed preliminary electronics for the COMET experiment [5]. The combined signal is the basic unit („trigger cell“) in the pre-trigger system. A typical waveform of the combined signal is shown in Figure 4.

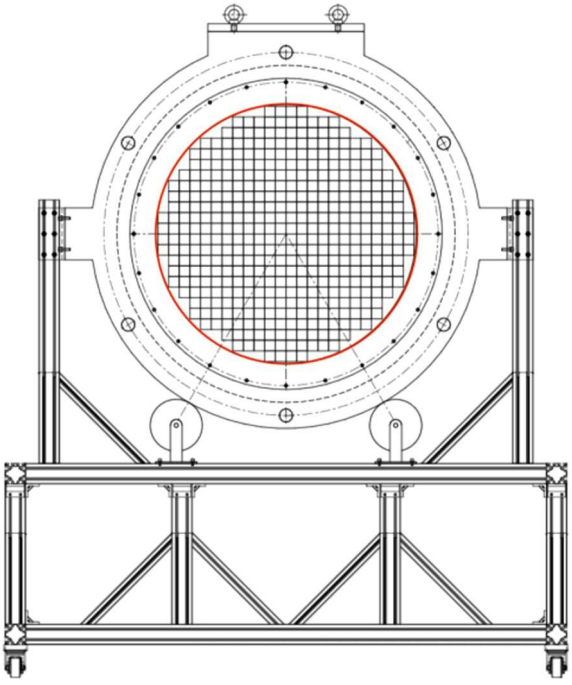

Figure 2. Schematic diagram of the electromagnetic calorimeter.

The EROS board [6] is used as a digitizing board for the calorimeter measurement path. Amplified and formed signals are recorded in a ring storage (DRS4 chip [7]) consisting of 1000 cells with a frequency of 1 GHz. Taking into account the time spent for the analysis of an input command from the trigger, the maximum travelling time window with respect to the event time, during which data is being stored and then correctly read, is ~ 900 ns.

2. Pre-trigger system

COMET trigger system flow diagram with a drift-tube detector and electromagnetic calorimeter is shown in Figure 5 [3,8]. The detector trigger system consists of a central trigger module (FC7) [9], control and synchronization boards (FCT), calorimeter pre-trigger (ECal Pretrigger) system, „fast“ trigger signal transfer module (FDB), pre-trigger of active cosmic radiation protection system (Cosmic trigger system) and trigger interface measurement electronic boards (Trigger I/F). Trigger signal is formed on the basis of calorimeter data. Each trigger-associated board is controlled by field programmable gate array (FPGA) to receive signals from the detector, perform digital data processing and transfer the formed parcel and solution to module FC7 via gigabit optical lines.

All trigger system and measurement path modules are synchronized by the central trigger (FC7) via the control and synchronization boards (FCT), which fulfil the interface function and connect all modules with the central trigger.

In the absence of an accelerator signal, FC7 sends clock rate for synchronization from the quartz oscillator placed on the board.

In all cases, the trigger signal is processed by the central trigger processor implemented in the FC7 FPGA.

Based on the foregoing, requirements for pre-trigger electronics of the electromagnetic calorimeter were defined:

1) energy resolution shall be better than 5 % with particle energy of about 105 MeV;

2) efficiency to effective events is at least 90 %;

3) delay of trigger signal arrival into the digitizing electronics from the event time shall be max. 900 ns.

2.1. General pre-trigger system structure

The COMET electromagnetic calorimeter will use 1920 crystals, therefore there are 480 trigger cells. It is technically difficult (virtually impossible) to conduct processing of all channels on one or even two circuit boards. In addition, the calorimeter has a fourfold symmetry. Therefore, the calorimeter is separated into our sectors in the pre-trigger, with one large board corresponding to each of them. On

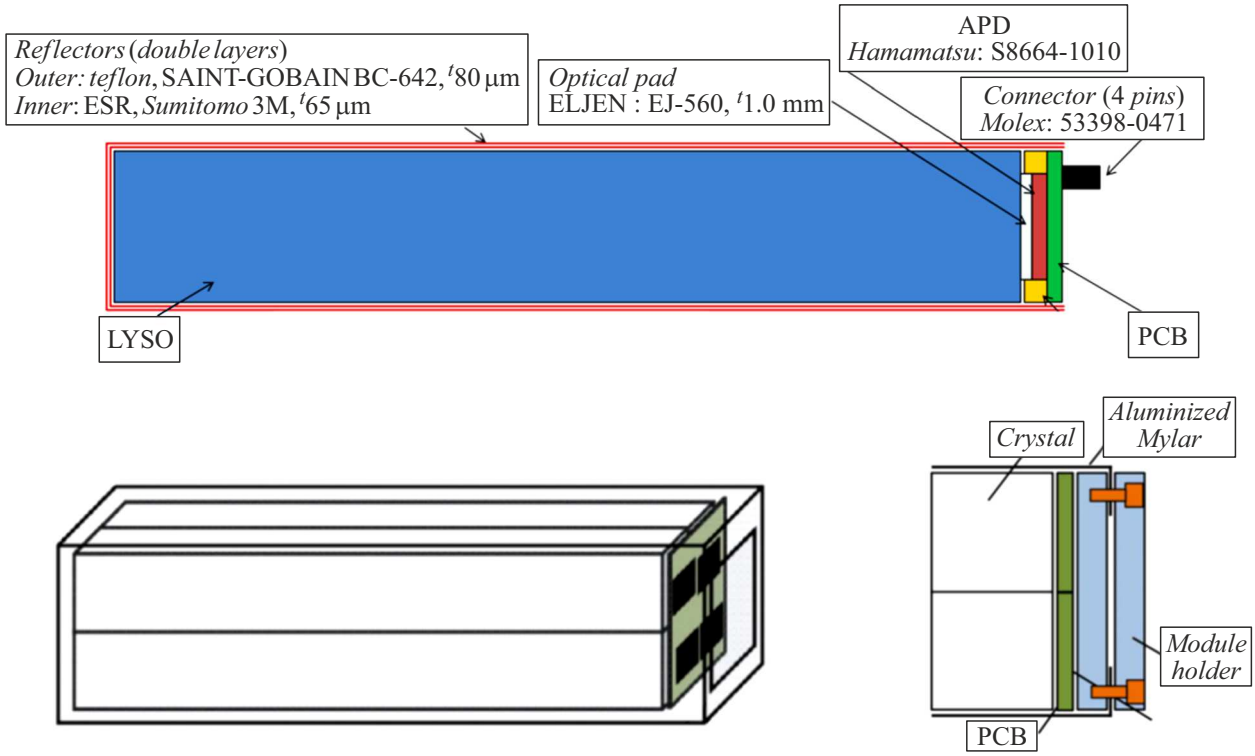

Figure 3. Top — one LYSO crystal with a photodiode and mounting board; bottom — 2 × 2 LYSO crystal module structure.

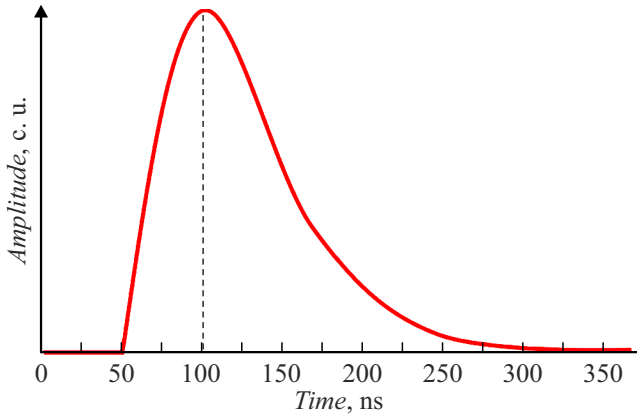

Figure 4. Typical combined signal waveform at the pre-trigger input.

the other hand, separation into six, eight and more trigger boards in the trigger is problematic because it would be necessary to duplicate and send a large amount signals between boards to overlap the sector boundaries, with each of the sectors processed by one board.

For overlapping of the borders between adjacent sectors, 12 digital signals are sent from a board to an adjacent one.

For analog-to-digital signal processing of analog signals from the calorimeter's preliminary electronics, 480/4 = 120 ADC (analog-to-digital converters) are placed on the electromagnetic calorimeter pre-trigger board. For physical problems, a 8 bit ADC is sufficient.

All digitized signals from the calorimeter are processed online in FPGA using the developed algorithm. When energy release is detected within the defined range $E_{\min} < E < E_{\max}$, 64 data bits are sent to the FC7 module using FCT to make a decision concerning recording of information about this event to the system of data collection from all detector systems.

To meet the requirements for time delay from the event time to arrival into the digitizing electronics that are applied to the trigger system, a double trigger model is implemented in the system to enable guaranteed reading of the measured data. The pre-trigger system additionally generates a „fast" trigger signal for the digitizing electronics and sends it via FDB directly to the digitizing boards to stop recording into the EROS/ROESTI cyclic memory.

For ease of setting and operation, it was decided to mount the analog section and digitizing components for calorimeter trigger signals on separate small 3U boards (digitizing board dimensions: 70 × 100 mm), and to perform digitized data processing on a motherboard that would be identical to a 6U busbar.

2.2. Engineering implementation of the pre-trigger system

ADC is one of the key components of digitizer boards. To reduce the time spent for discretization of analog inputs

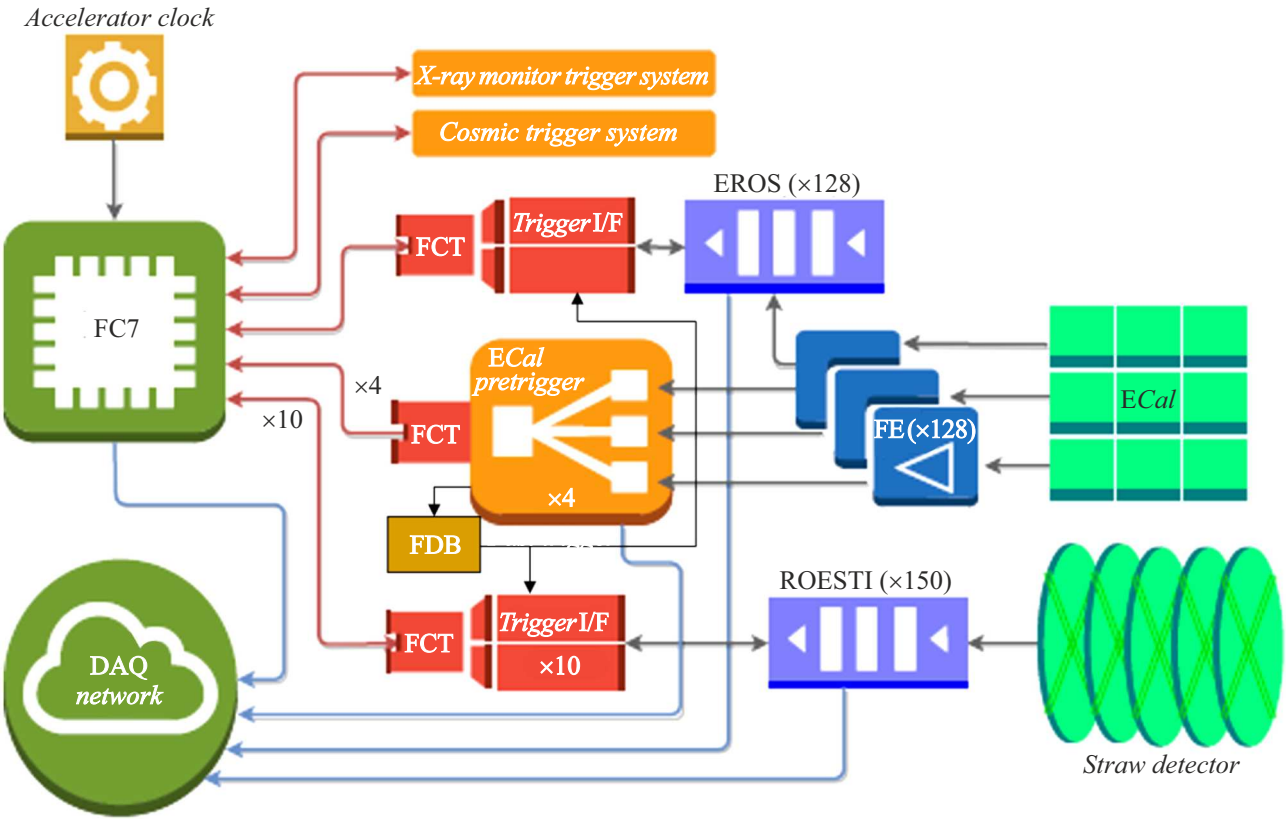

Figure 5. COMET trigger system flow diagram with a drift-tube detector and electromagnetic calorimeter.

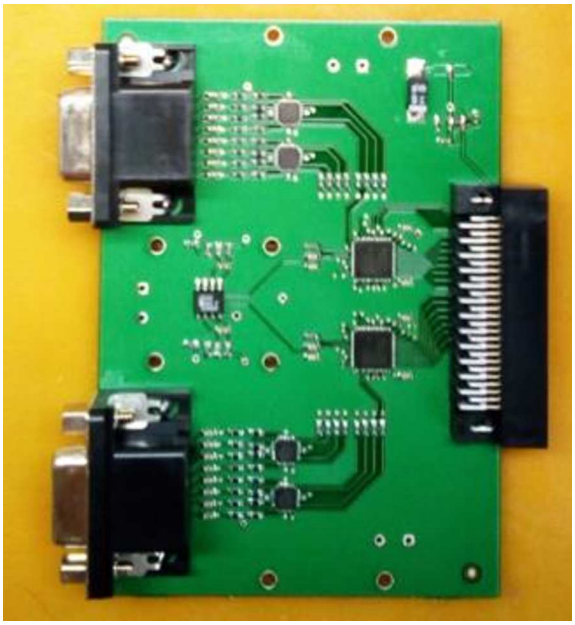

Figure 6. Electromagnetic calorimeter pre-trigger digitizing board.

from preliminary electronics boards, but to avoid high loss of resolution (reduction of the number of bits of ADC), Analog Device AD9287 four-channel ADCs with a sampling rate of 80 MHz and 8-cycle conversion time (100 ns) were used for the digitizing boards. Each digitizing board contains two such ADCs (Figure 6). A total of 16 digitizing boards may be mounted in a motherboard (Figure 7).

A digital pre-trigger assembly is based on AMD (Xilinx) Virtex-4 series FPGA. Flow diagram of the internal pre-trigger FPGA structure is shown in Figure 8.

Digital section of the pre-trigger motherboard unit fulfils the following tasks:

- receives data from ADC crystals with a preset clock rate;
- loads reference constants into ADC control registers and FPGA internal registers when power supply is turned on;
- performs real-time data processing procedures for data received from all 128 channels;
- generates a „fast“ trigger signal [10] for measurement path digitizing boards;
- transfers trigger information via FCT to FC7 for final decision making.

All digitized signals arriving to the pre-trigger mother-board from the calorimeter are processed online in FPGA using the developed algorithm.

All pre-trigger components underwent stability testing under high irradiation up to 2 kGy and of 10^{12} neutron/cm^2 flux. Testing results have shown that all components are

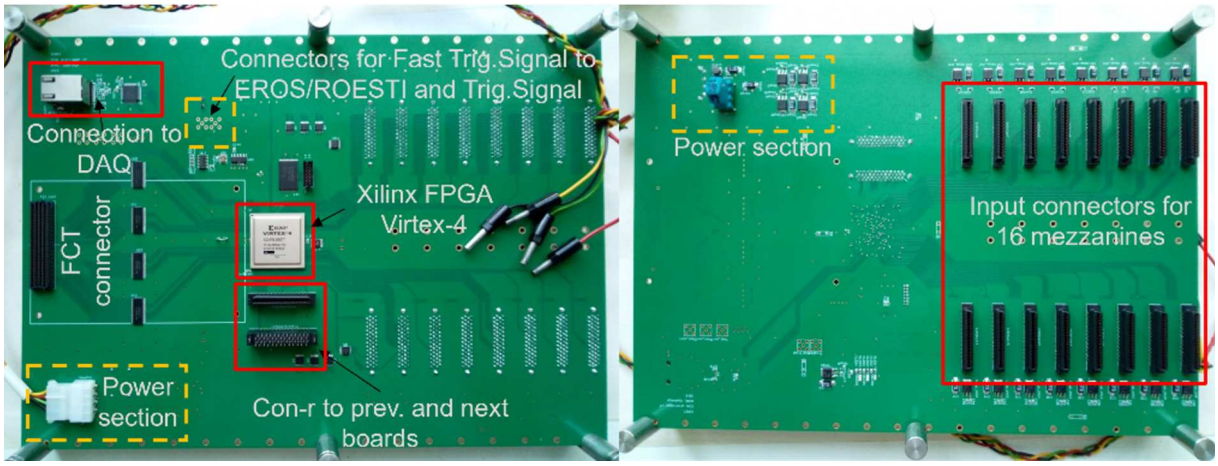

Figure 7. Electromagnetic calorimeter pre-trigger motherboard. Left — bottom view; right — top view.

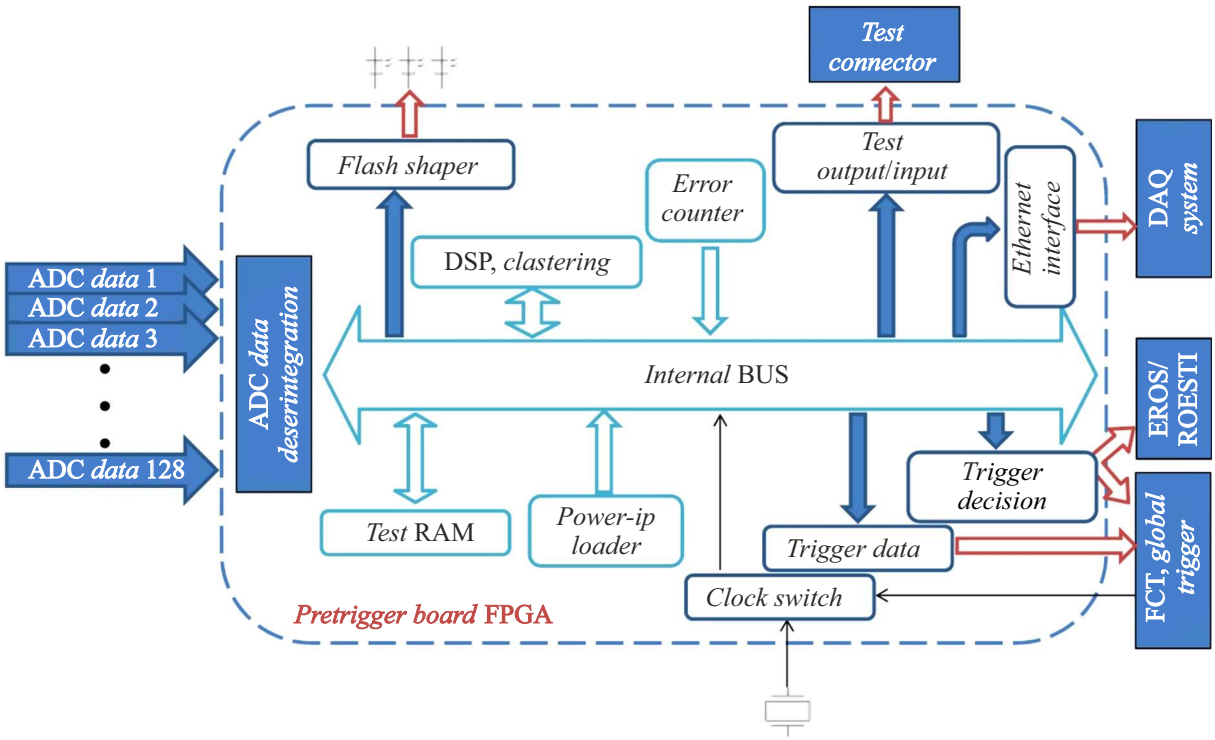

Figure 8. Flow diagram of the internal pre-trigger FPGA structure for the electromagnetic calorimeter.

resistant to irradiation up to 2 kGy and 10^{12} neutron/cm^2 flux [11,12] and satisfy the experiment requirements.

3. Cluster searching algorithm

With energies about 100 MeV, the electromagnetic shower induced by an arriving particle will be distributed over several calorimeter crystals. To recover full energy of particles entering the electromagnetic calorimeter, energy release shall be summed up over several crystals adjacent to the crystal with a maximum energy release. When determining the cluster energy in real time, only trigger cell signals are accessible for the trigger, therefore it is important to choose an optimum number of trigger cells, which shall be assigned to one cluster for energy summation, to meet the pre-trigger electronics requirements.

Upon completion of simulation [13], it was decided to use the trigger cell cluster size of 2×2 in the electromagnetic calorimeter pre-trigger.

For the 2×2 cluster case, the energy release determination algorithm was as follows: first, energy release was summed up over all possible combination of 2×2 trigger

cells as shown in Figure 9. Then, a sum with the maximum energy release was determined.

3.1. Hardware implementation of the algorithm

The developed clustering algorithm was implemented on the FPGA basis and all digitized input channel data are analyzed online and simultaneously:

- first, the pedestal value is subtracted from the received signals, slight smoothing integration takes place through summation (averaging) of two successive values with a time constant of 25 ns;
- after that, input signals are summed up into trigger groups consisting of 4 trigger cells according to the groups preliminary prescribed in tables;
- then, the summation result is forwarded to amplitude discriminators and compared with the pre-defined threshold level. When a high level signal (logical „1“) appears at the discriminator output, a threshold crossing flag is „enabled“ and the grouped amplitudes are allowed to arrive at trigger group and cluster amplitude search submodules (maximum amplitude groups). At the same time, a „fast trigger“ signal is formed and sent to the digitizing boards from the measurement channel with a minimum delay;
- trigger group amplitude is defined by comparing the combined amplitude value delayed for one cycle with the current value, i.e. received at this moment. As soon as the currently received value decreases below the delayed value, the delayed combined amplitude value is taken as the trigger group amplitude. At the moment when the trigger group amplitude has been determined, an appropriate „flag“ is generated for this group, and a corresponding group value is recorded into a register;
- cluster search algorithm checks all possible trigger group combinations and compared their combined amplitudes in pairs as shown in Figure 10. 16-bit registers, into which combined amplitude values (10 bit) and trigger group No. (6 bit) are recorded, are used for comparison. Data from a channel with the largest combined amplitude is transferred to the next comparison stage; after the final comparison, amplitude and No. of the group with the maximum energy release in this cross-section will be known.
- after determining the amplitude and corresponding No. of the trigger group, a parcel is formed for the FC7 board to take a final decision on whether to generate a recording signal for this event according to all received data;
- the whole system is reset in the following cases:
  - the discriminator threshold crossing „flag“ is enabled, but there was no amplitude determination „flag“ for this channel or central trigger signal during 1 μs (variable and may be changed) after that;
  - all „flags“ are enabled and both trigger signals are formed. After that, the algorithm is ready for work again in $\sim$ 60 ns.

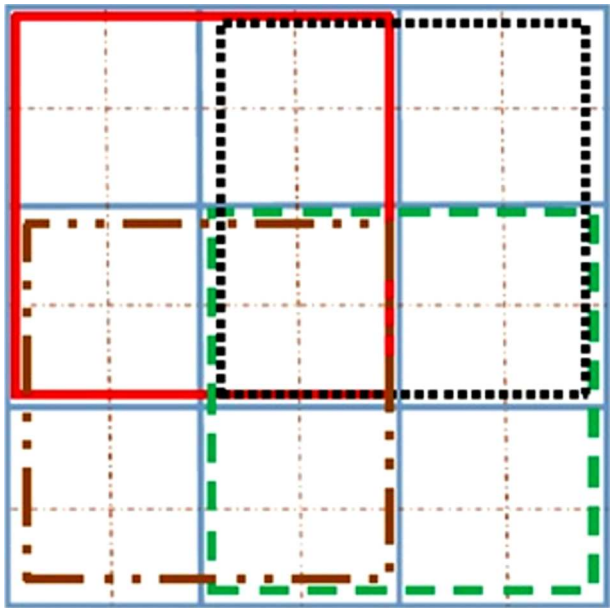

Figure 9. Summation over all possible combinations of 2×2 trigger cells.

4. Measurement of energy resolution and pre-trigger system efficiency

The pre-trigger system was tested on an extracted electron beam (Tohoku University, Sendai, Japan). A calorimeter prototype consisting of 64 crystals, 4 preliminary electronics boards and pre-trigger electronics (2 digitizing boards and a motherboard) was used for testing.

The test included 10 starts (5 starts from the calorimeter trigger system and 5 starts from an external system for efficiency measurement) consisting of $\sim$ 20 events each. Pre-trigger efficiency was calculated from the relation between the number of events detected by the external system and events detected by the calorimeter trigger system. General pre-trigger system efficiency with energy release above 30 MeV was 99.4 %, with energy release above 40 MeV was 99.7 %. Trigger system energy resolution for the recorded starts at 105 MeV was approximately 4.5 %, which is very close to the value obtained from offline data processing in the measurement channel — 4.4 % [3] and fully meets the requirements applied to the system. For more detailed description of the experimental testing procedure and findings for the pre-trigger system see [10,13,14].

5. Measurement decision-making time and trigger generation delay

One of the most important requirements applied to the electronics being developed is effective event recording efficiency, background event suppression and delay of trigger arrival at the digitizing electronics.

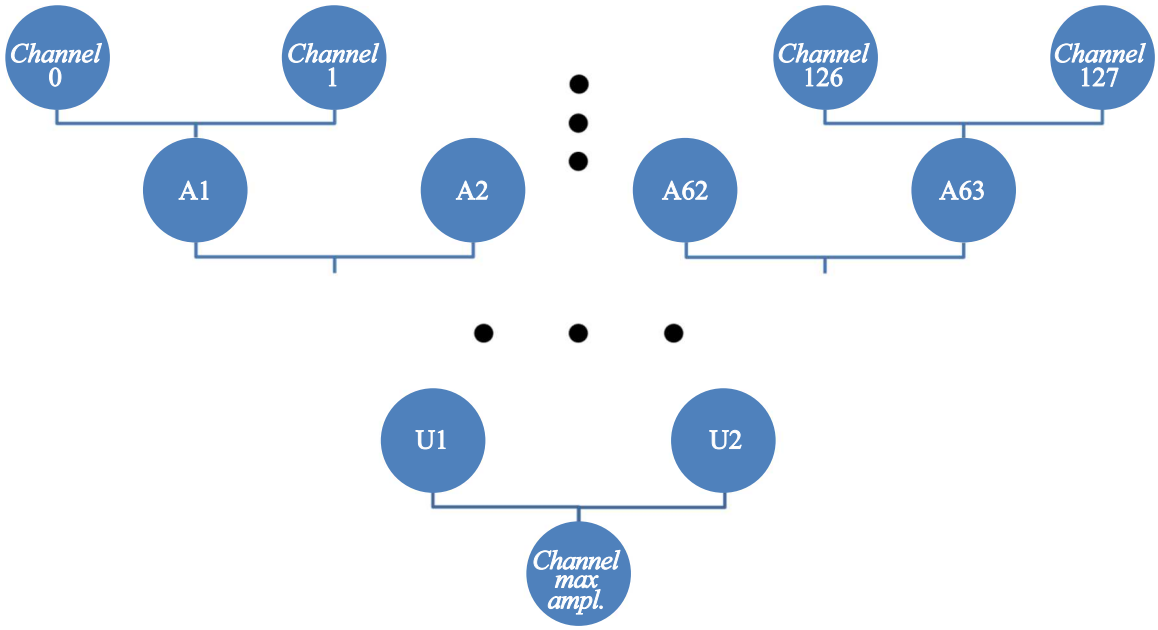

Figure 10. Search for a trigger group with the maximum energy release in the given cross-section.

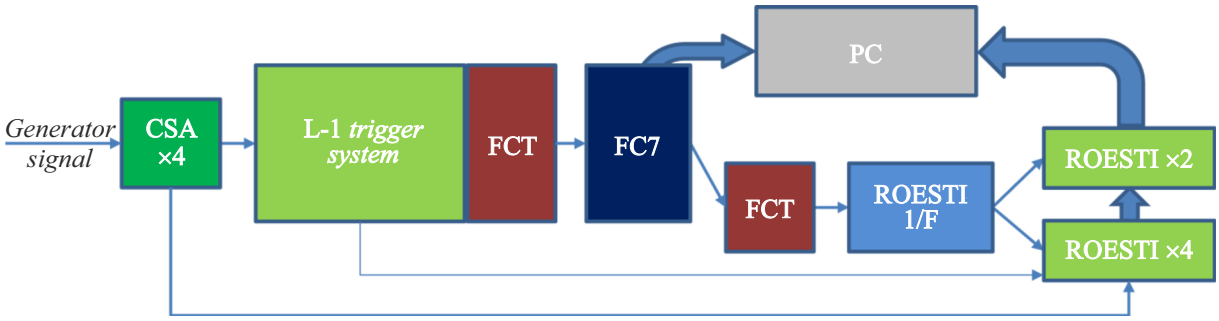

Figure 11. Functional flow diagram of the equipment for decision-making time and trigger signal generation delay measurement.

To check the trigger arrival delay at the digitizing modules of the measurement channel, a bench was assembled, whose functional flow diagram is shown in Figure 11. Full trigger path of the electromagnetic calorimeter underwent a series of tests for measuring the trigger generation time and arrival delay at the digitizing boards of the electromagnetic calorimeter, and the drift tube system was also tested.

Tektronix AFG3102 arbitrary waveform oscillator was used as a signal source. A signal from the oscillator was applied to the calibration input of the preliminary electronics boards of the electromagnetic calorimeter, where it was amplified and sent via two lines:

- to the EROS digitizing boards of the measurement channel;
- to the pre-trigger system input (L-1 Trigger system), where voltage level matching was performed between the preliminary electronics boards and pre-trigger digitizing boards for further discretization using ADC.

Digitized 8-bit signal values in the LVDS sequential form arrived at the pre-trigger FPGA on the motherboard, where the digitized data was further processed in steps described in Section 3.1.

Figure 12 shows an oscilloscope waveform in key points of the electronic path of the electromagnetic calorimeter:

- green generator signal supplied to the preliminary electronics board input and taken as the reference point of time measurements;
- pink formed „fast“ trigger sent directly to the EROS/ROESTI interface boards via the level converter;
- yellow EROS cyclic memory writing stop signal;
- cyan data reading trigger generated by FC7 at the EROS input.

As can be seen from the waveform, the final delay from the event time to data reading trigger arrival from the central trigger to the digitizing boards of the measurement path is max. 900 ns. Data received by the digitizing board of the

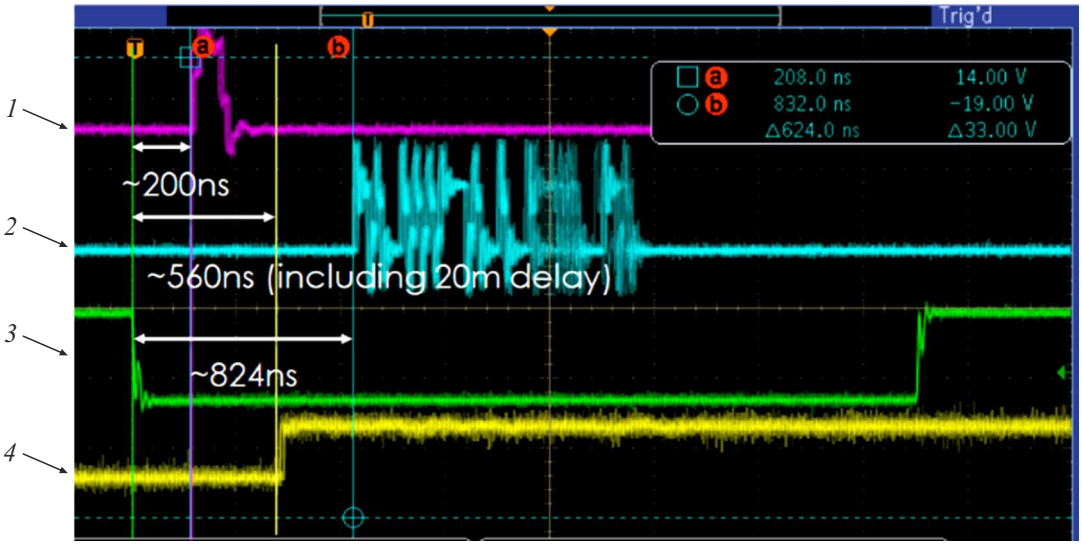

Figure 12. Oscilloscope waveform in key points of the electronic path of the electromagnetic calorimeter: *1* — „fast“ trigger, *2* — reading trigger generated by FC7 at the EROS input, *3* — oscillator output, *4* — central trigger at the EROS input.

measurement path from the preliminary electronics were successfully read in the data collection system.

Conclusion

Pre-trigger logic algorithm was developed, simulated and tested in the electronics on the bench and in real events. The test has shown that the algorithm worked properly. Trigger system energy resolution of approximately 4.5 % was obtained with the extracted electron beam for the recorded starts at 105 MeV, which is very close to the value obtained from offline data processing in the measurement channel — 4.4 % and fully meets the requirements applied to the system.

Electronics debugging and bench testing procedures, and the appropriate software have been developed. All electronic modules and units have been debugged and checked for using in the experiment. Experimental electronics monitoring and online control techniques have been developed.

To date, the electromagnetic calorimeter pre-trigger system has been developed, fabricated, tested and is ready for starting the experiment.

Conflict of interest

The authors declare no conflict of interest.

References

[1] Y. Kuno (COMET collaboration). Prog. Theor. Exp. Phys., **022C01**, 1 (2013). DOI: 10.1093/ptep/pts089
[2] Y. Uchida (COMET collaboration). J. Instrumentation, **9** (9), C09008 (2014). DOI: 10.1088/1748-0221/9/09/C09008
[3] R. Abramishvili (COMET collaboration). Prog. Theor. Exp. Phys., **2020** (3), 033C01 (2020). DOI: 10.1093/ptep/ptz125
[4] Kou Oishi (COMET collaboration). JPS Conf. Proc., **8**, 025014 (2015). DOI: 10.7566/JPSCP.8.025014
[5] Yu.V. Yudin, D.N. Grogoriev, L.B. Epshtein. Avtometriya, **54** (2), 113 (2018) (in Russian).
[6] K. Ueno, E. Hamada, M. Ikeno, S. Mihara, H. Nishiguchi, M. Shoji, T. Uchida, Y. Fujii, R. Kawashima, K. Oishi, J. Tojo, Y. Nakazawa, H. Yoshida. PoS, EPS-HEP2019, **364**, (2020). DOI: 10.22323/1.364.0175
[7] S. Ritt. Nucl. Instr. Meth. A, **518** (1−2), 470 (2004). DOI: 10.1016/j.nima.2003.11.059
[8] L.B. Epshteyn (COMET collaboration). JINST, **12**, C01064 (2018). DOI: 10.1088/1748-0221/12/01/C01064
[9] M. Pesaresi, M. Barros Marin, G. Hall, M. Hansen, G. Iles, A. Rose, F. Vaseyb, P. Vichoudis. J. Instrumentation, **10** (3), C03036 (2015). DOI: 10.1088/1748-0221/10/03/C03036
[10] D.N. Grigoriev, L.B. Epshteyn, Dz.V. Shoukavy. Moscow Univer. Phys. Bull., **79** (1), S1 (2024).
[11] L.B. Epshteyn, R.R. Akhmetshin, D.N. Grigogiev, Dz.V. Shoukovy, Yu.V. Yudin. *The electronics for the electron calorimeter of the COMET experiment*, IEEE Nuclear Science Symposium and Medical Imaging Conference, 2018, 2019. DOI: 10.1109/NSSMIC.2018.8824666
[12] Yu. Nakazawa, Yu. Fujii, E. Gillies, E. Hamada, Yo. Igarashi, M.J. Lee, M. Moritsu, Yu. Matsuda, Yu. Miyazaki, Yu. Nakai, H. Natori, K. Oishi, A. Sato, Yo. Uchida, K. Ueno, H. Yamaguchi, B. Yeo, H. Yoshida, J. Zhang. Nucl. Instrum. Meth. A., **955**, 163247 (2020). DOI: 10.1016/j.nima.2019.163247
[13] D.V. Shelkovy, D.N. Grogoriev, L.B. Epshtein, Yu.V. Yudin. Izvestiya NAN Belarusi. Seriya fiziko-matematicheskikh nauk, **160** (56), 1 (97) (in Russian).
[14] L.B. Epshtein, R.R. Akhmetshin, D.N. Grogoriev, V.F. Kazanin, A.S. Melnik, D.V. Shelkovy, Yu.V. Yudin. Sibirskiy fiz. zhurn. Seriya: Fizika vysokikh energii, uskoritelei i vysokotemperaturnoi plazmy, **12** (4), 5 (2017) (in Russian).

Translated by E.Ilinskaya